nature cell biology

DOI: 10.1038/ncb2428

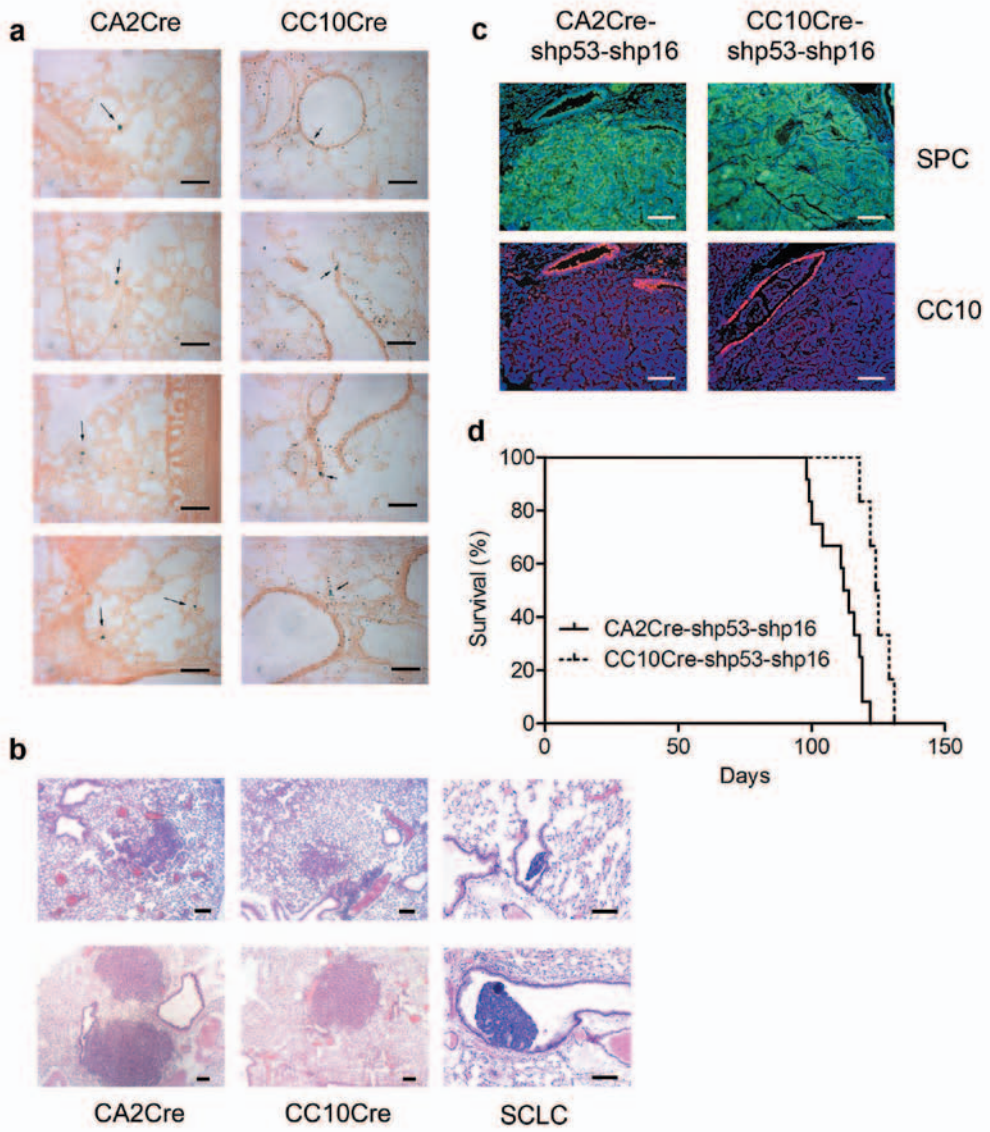

Figure S1 CA2Cre and CC10Cre lentiviruses initiated lung adenoma by targeting alveolar epithelial cells. (**a**) Rosa26^{lacZ} reporter mice were infected intra-tracheally with CA2Cre or CC10Cre lentiviruses. β-galactosidase expression was examined by X-gal staining 14 days after the infection. Cells infected with lentiviruses and had Cre expression were stained blue (arrows). (**b**) Kras^{G12D} mice were infected with CA2Cre or CC10Cre lentiviruses. Lung tumours were examined 2 (top) or 4 (bottom) months after the infection. Lesions were found only in the alveoli. In contrast, in a small cell lung cancer model (SCLC, Xia et al. unpublished), lesions were found exclusively in the bronchioles. (**c**) Kras^{G12D} mice were infected with CA2Cre-shp53-shp16 or CC10Cre-shp53-shp16 lentiviruses. Tumours were typical adenocarcinomas with SPC positive and CC10 negative staining. Scale bars, 100 μm. These two groups of mice didn't show big difference in median survival time, n=12 and 6 respectively (**d**).

© 2012 Macmillan Publishers Limited. All rights reserved.

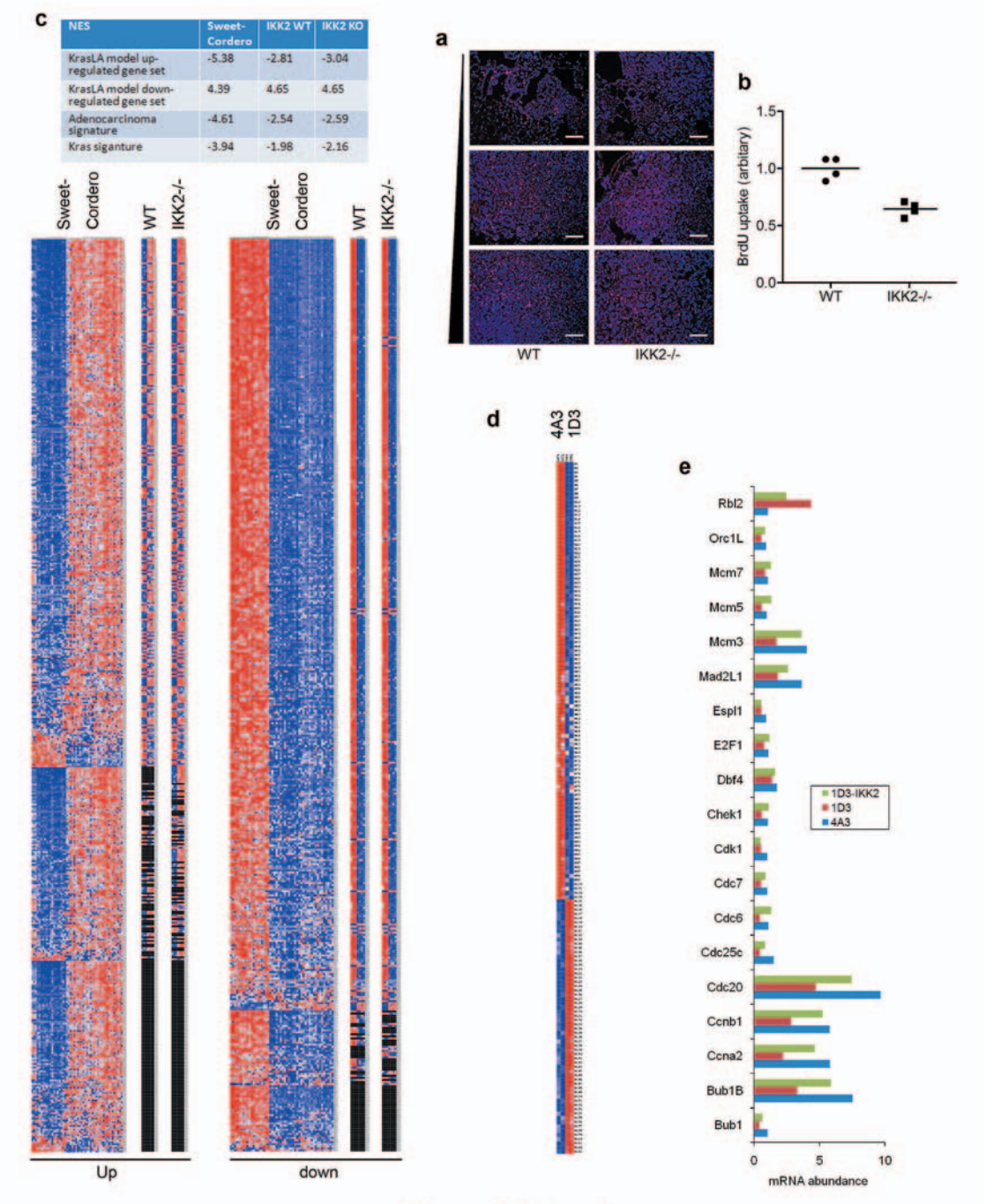

NES	Sweet-Cordero	IKK2 WT	IKK2 KO
KrasLA model up-regulated gene set	-5.38	-2.81	-3.04
KrasLA model down-regulated gene set	4.39	4.65	4.65
Adenocarcinoma signature	-4.61	-2.54	-2.59
Kras siganture	-3.94	-1.98	-2.16

Figure S2 Reduced proliferation was found in IKK2-/- tumour. (**a**) Ki-67 staining was done on tumour sections of different stages (from top to bottom: early to late stages). Compared to WT counterparts, IKK2-/- tumours had lower Ki-67 positive percentage. Scale bars, 100 μm. (**b**) BrdU uptake was measured in a collection of cell lines derived from WT and IKK2-/- tumours. The results indicated lower proliferation rate in IKK2-/- cells. (**c**) Kras signature of WT and IKK2-/- tumours. Comparisons of normal (N) versus tumour (T) samples of up- or down- regulated KrasLA genes as defined by Sweet-Cordero are shown by heat maps. Red indicates higher expression levels than blue. Each row is one gene and each column is one array. Rows are normalized to zero with a variance of one for display purposes. Genes are first segregated by their presence in the data sets, and then are ordered by decreasing significance as determined by GSEA. Missing values are either due to lack of mapping or in most instances insignificant differential gene expression, are represented as black and values close to zero are in white. Normalized Enrichment Scores (NES) from GSEA are shown on the top. Positive numbers indicate enrichment of gene set in normal lung tissue while negative numbers indicate enrichment in tumour. Overall, scores of WT and IKK2-/- tumours are very close, indicating that both tumours are lung adenocarcinomas with Kras signature. (**d**) Differential gene expression between WT and IKK2-/- tumours. Comparison of WT (4A3) and IKK2-/- (1D3) tumour cell lines of NF-κB genes as defined by Gilmore. Total 103 genes are up-regulated in WT cells. NES for NF-κB target genes is 2.41. (**e**) Nineteen cell-cycle related genes that showed changes in the microarray analysis (both tumours and cells) were picked for further verification. RNAs from WT (4A3), IKK2-/- (1D3) and IKK2 reconstitution (1D3-IKK2) cells were analyzed. IKK2 reconstitution in 1D3 cells restored the gene expression pattern. Results are shown as average of two biological replicates.

© 2012 Macmillan Publishers Limited. All rights reserved.

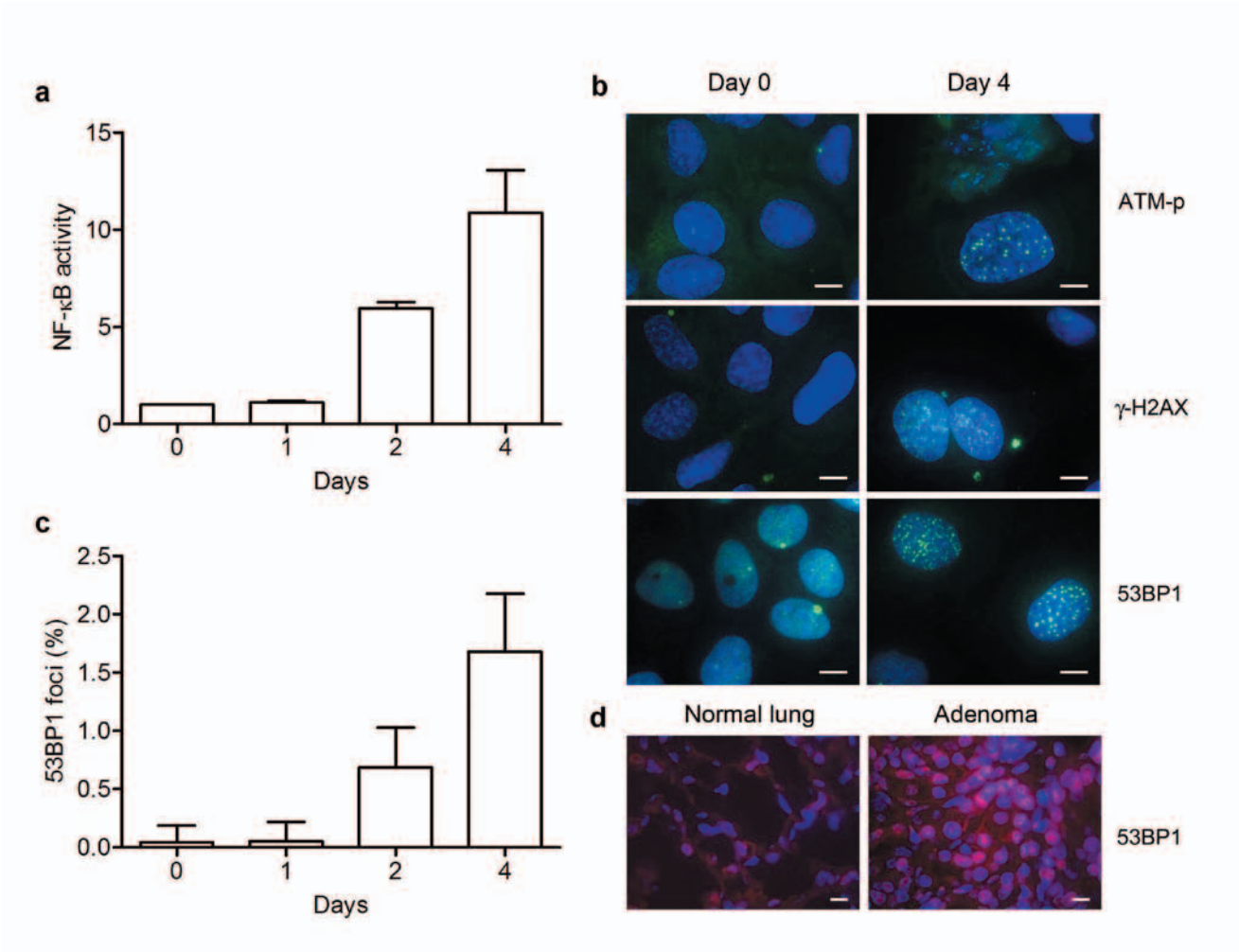

Figure S3 $Kras^{G12D}$ induced DNA damage response and NF-κB activation. (**a**) $Kras^{G12D}$ was expressed under the regulation of tetracycline responsible elements (TRE) in U2OS cells for different time. NF-κB activity was measured by luciferase reporter assay. Error bars, s.d. (n=4 biological replicates.) (**b**) DNA damage response was shown by immunostaining of ATM-p, phos-γH2A and 53BP1 foci. (**c**) Quantification of 53BP1 foci positive cells at different time point. Error bars, s.d. (n=10 random fields.) (**d**) Immunostaining of 53BP1 in early lung tumour lesion induced by CA2Cre-shp53 lentivirus. Scale bars, 10 μm.

© 2012 Macmillan Publishers Limited. All rights reserved.

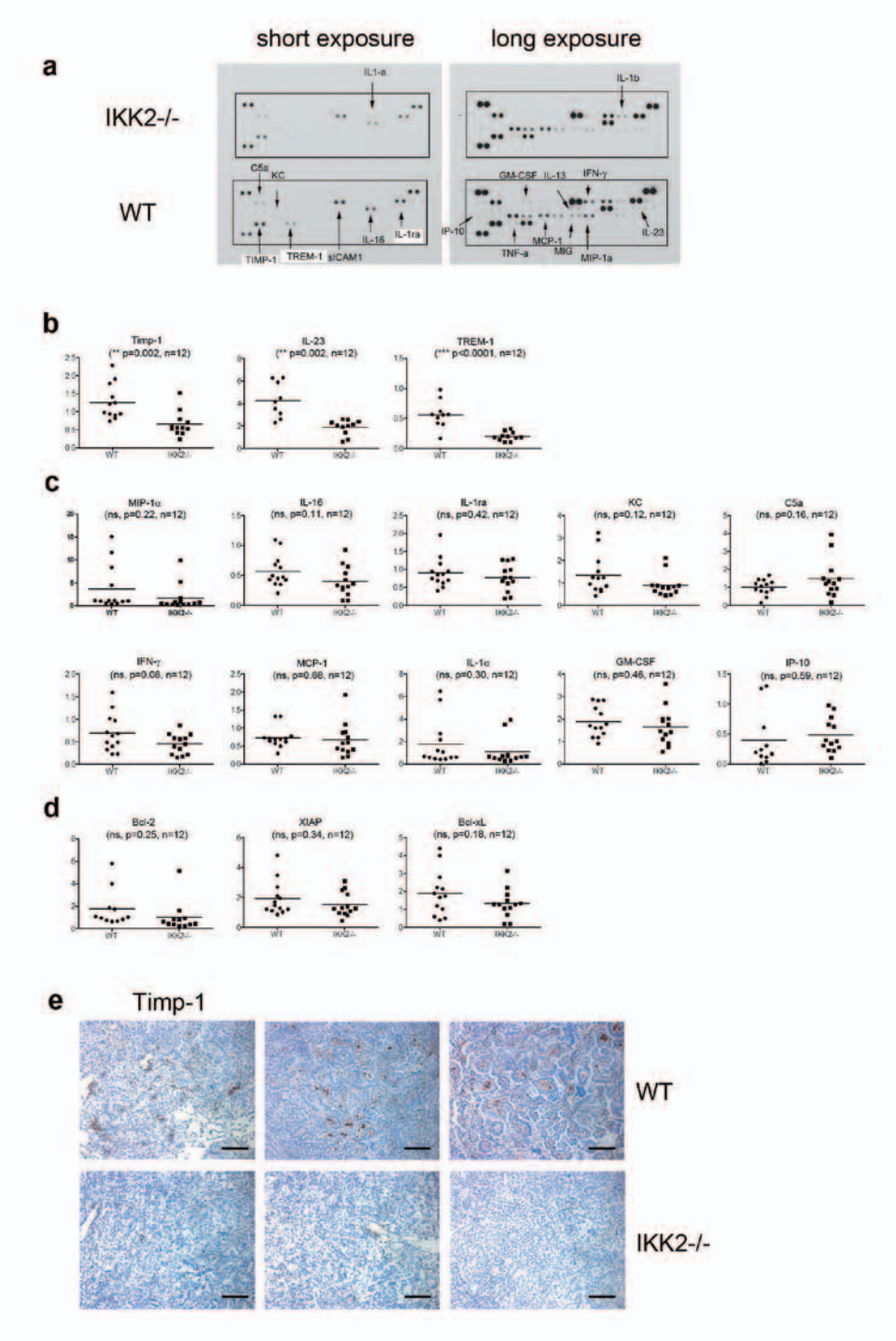

Figure S4 Cytokine array analysis of WT and IKK2-/- tumours identified Timp-1. (**a**) Primary tumours of similar size were precisely dissected and whole lysates were used for cytokine array. Visible dots corresponding to different cytokines were quantified with Image J. (**b,c**) Those genes showed difference in cytokine array were further verified by quantitative RT-PCR with more tumour samples. Three genes were confirmed lower in the IKK2-/- tumours (**b**), while other genes showed no statistical difference (**c**). (**d**) Anti-apoptotic genes regulated by NF-κB didn't show difference between WT and IKK2-/- tumours. (**e**) Timp-1 expression was examined by immunohistochemistry in WT and IKK2-/- tumours at different stages (from left to right: early to late stages). Scale bars, 100 μm.

© 2012 Macmillan Publishers Limited. All rights reserved.

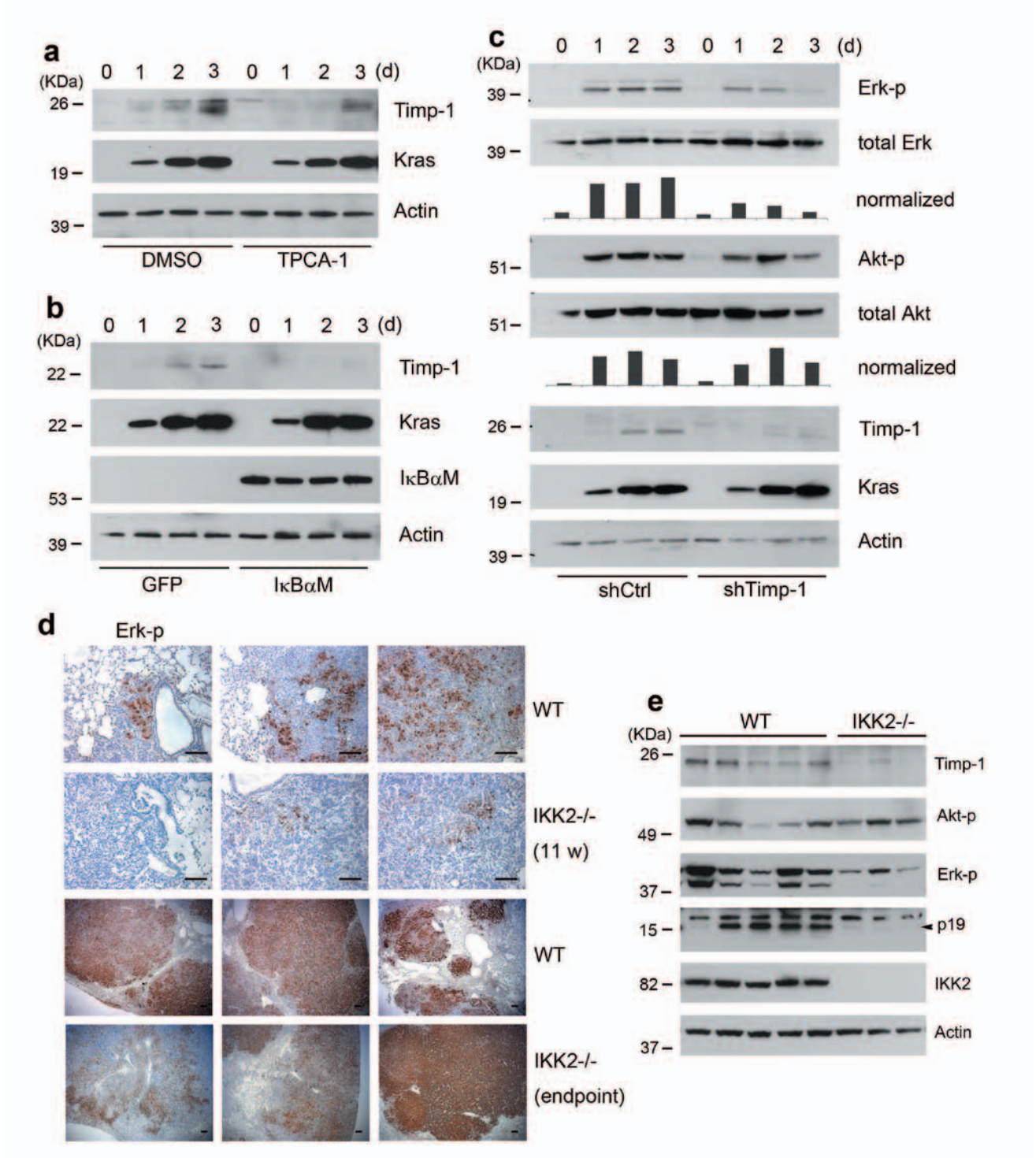

Figure S5 Timp-1 expression is required for maintaining high Erk activation. (**a,b**) TRE-Kras^{G12D} expression in U2OS cells induced Timp-1 expression via NF-κB, which was abolished by IKK2 inhibitor TPCA-1 or IκBαM super repressor. (**c**) Erk but not Akt phosphorylation was attenuated by shTimp-1, indicating the role of IKK2/Timp-1 in maintaining high Erk activation downstream of Kras. (**d**) Erk phosphorylation was examined in WT and IKK2-/- tumours at 11 weeks and endpoint. In 11-week WT samples, Erk-p was found in mosaic pattern. Notice that Erk-p was visible even in some early lesions. In contrast, 11-week IKK2-/- samples had very little positive staining. In endpoint samples, IKK2-/- tumours had slightly lower staining than WT, however very strong staining was also found in some tumours. These tumours might have obtained certain mutations that could bypass the requirement of IKK2/Timp-1 for maintaining high Erk activation. Scale bars, 100 μm. (**e**) Stable cell lines derived from IKK2-/- tumours showed lower Timp-1 expression and Erk phosphorylation, compared to WT counterparts.

© 2012 Macmillan Publishers Limited. All rights reserved.

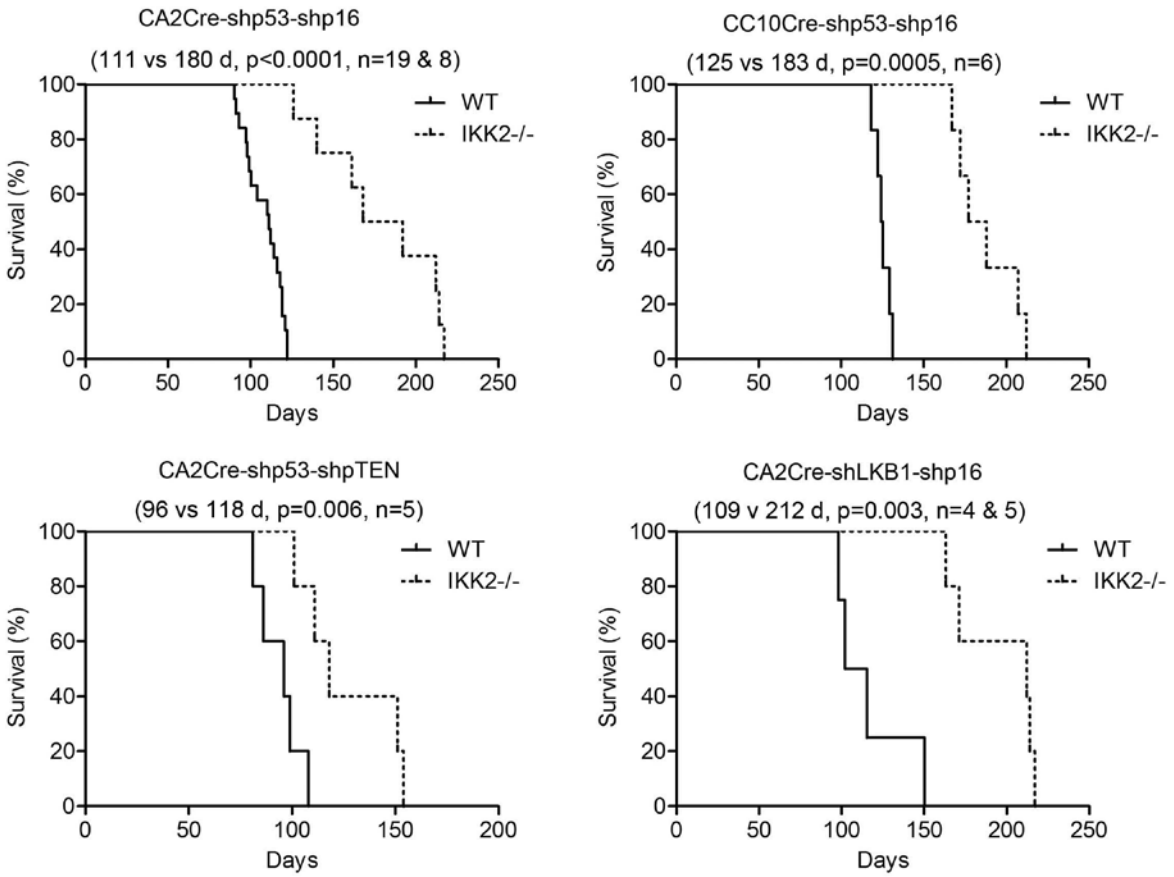

Figure S6 IKK2 depletion in tumour cells prolonged median survival time. Tumours were induced in $Kras^{G12D}$ mice by lentiviral vectors carrying different mutations. In all cases, IKK2 depletion in tumour cells increased median survival time, indicating the role of NF-κB and IKK2 in tumour progression is not limited to tumours with certain mutations.

© 2012 Macmillan Publishers Limited. All rights reserved.

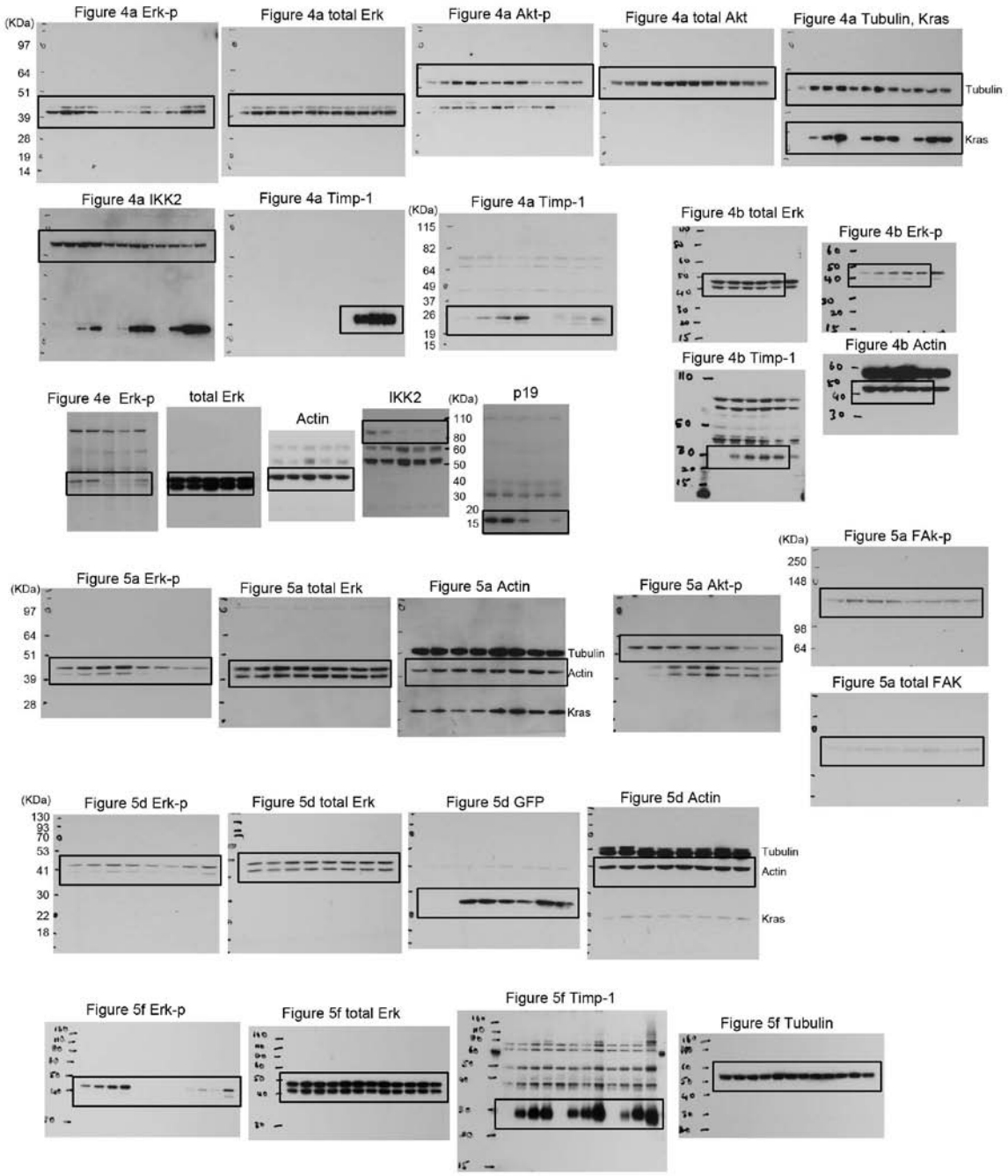

Figure S7 Full scans of the immunoblotting analysis in Figure 4 and Figure 5. Cropped regions are indicated by boxes.

© 2012 Macmillan Publishers Limited. All rights reserved.

Supplementary Table legends

Table S1 Normalized Enrichment Scores (NES) comparing WT and IKK2-/- tumours. Positive numbers indicate enrichment of gene set in WT tumours, while negative numbers indicate enrichment in IKK2-/- tumours. Cell cycle related terms are the major changes, which are consistent with the high proliferation rate found in WT tumours.

Table S2 Full list of primers used in quantitative RT-PCR.

© 2012 Macmillan Publishers Limited. All rights reserved.